JOURNAL OF MATERIALS SCIENCE 30 (1995) 5576–5580

Analysis of microhardness data in $Tl_xIn_{1-x}Se$

I. Y. YANCHEV, E. P. TRIFONOVA
Faculty of Physics, St Kliment Ohridski University of Sofia, 1126 Sofia, Bulgaria
CH. KARAKOTSOU, A. N. ANAGNOSTOPOULOS, G. L. BLERIS
Solid State Section, Physics Department, Aristotle University of Thessaloniki, 54006 Thessaloniki, Greece

Microhardness measurements have been performed on $Tl_xIn_{1-x}Se$ semiconductors ($x = 0.0, 0.2, 0.3 \ldots 1.0$). The microhardness, H, as a function of x shows a maximum at x ca. 0.5. A statistical evaluation of the obtained results leads to a log-normal distribution of the microhardness rather than, as expected, a polynomial one.

1. Introduction

$TlInSe_2$ and some related compounds are ternary semiconductors with very unusual electrical properties. In some recent publications [1–4] their S-type current–voltage characteristic and the chaotic voltage oscillations appearing in the corresponding NDR-region are examined. In another report the influence of the stoichiometry is examined [5], i.e. how changes of x in the system $Tl_xIn_{1-x}Se$ affect the non-linear electrical properties. However, the mechanical properties of the $Tl_xIn_{1-x}Se$ compounds had not been examined in a systematic way. The aim of the present work is to report some data concerning the dependence of microhardness on x.

2. Experimental procedure

The samples used for the microhardness measurements were $Tl_xIn_{1-x}Se$ (with $x = 0, 0.2, 0.3 \ldots 1.0$). These compositions form the InSe–TlSe quasi-binary cross-section of the concentration triangle of the ternary system In–Tl–Se (Fig. 1). The crystals were prepared by crystallization from stoichiometric melts in evacuated ampoules.

Being too small (a few cubic millimetres) and of irregular shape, the samples were encapsulated in dental resin (Kallocryl CP-rz), enabling easy handling. After hardening, which took 24 h, the capsules were mechanically polished with 5 mm alumina powder until flat surfaces of the samples were obtained. Microscopic observation revealed that these surfaces consisted of lapped and cleaved areas. Indentations were made on both areas.

Microhardness measurements were carried out at room temperature with PMT-3 microhardness tester [6]. The Vickers diamond indentor (a square-based pyramid) was maintained in contact with the sample's surface for 60 s. This was an unusually long time, but preliminary measurements showed that shorter contact times gave unstable indentations. The indentor was loaded with 10 g. The indentation marks produced were of irregular contours; cracks could be seen around the indentations due to material brittleness.

The microhardness of the $Tl_xIn_{1-x}Se$ samples as a function of x is presented in Fig. 2. In order to reduce experimental uncertainty, at least five, and typically 10, indentations on a given sample were produced. It can be seen that the dependence was characterized by a maximum at $x = 0.3$–0.5. TlSe is harder than InSe, a fact consistent with its broader gap. The relatively large scattering of experimental data is presumably due to: (1) the samples not being monocrystalline; and (2) the indentations having irregular contours. It can be seen that the scattering of the data is smaller in the case of the binary compounds.

According to the Kurnakov rules for the variation of hardness with composition in metal solid solutions [7]:

1. The formation of solid solutions is accompanied by an increase in hardness.
2. The variation of hardness over a continuous compositional range of solid solutions yields a continuous curve possessing a maximum.

Later, Goryunova *et al.* [6] showed that these rules were also valid for semiconductor solid solutions. Hence, our results represent another verification of Kurnakov rules. Goryunova *et al.* assumed that their behaviour might be due to "healing of defects" which took place in certain alloy compositions. But the following consideration may also be taken into account: production of an indentation is accompanied by material transfer to the adjacent parts of the crystal. This transfer is facilitated by the presence of defects, e.g. dislocations – the bigger the dislocation density, the softer the material. On the other hand, it is known that the dislocation density in some materials can be reduced by doping, as in the case of GaAs and InP doped with Zn, S, Te, Al or N [8, 9]. Several explanations have been proposed to aid understanding this experimental fact. One of them (the so-called "pinning effect") is based on the assumption that dislocations

0022–2461

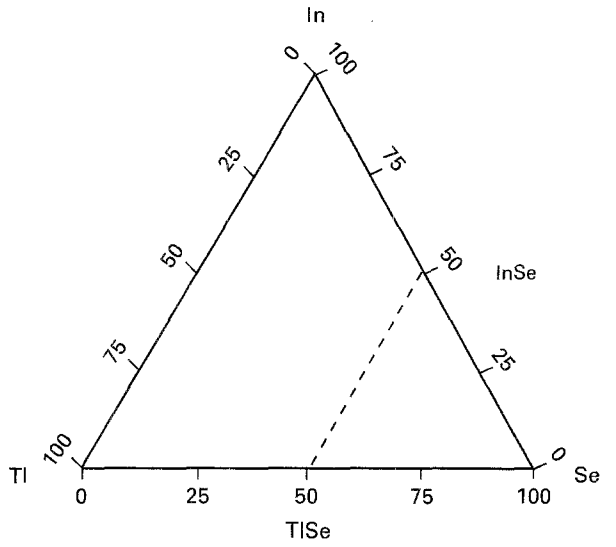

Figure 1 The In–Tl–Se concentration triangle with the InSe–TlSe quasibinary cross-section.

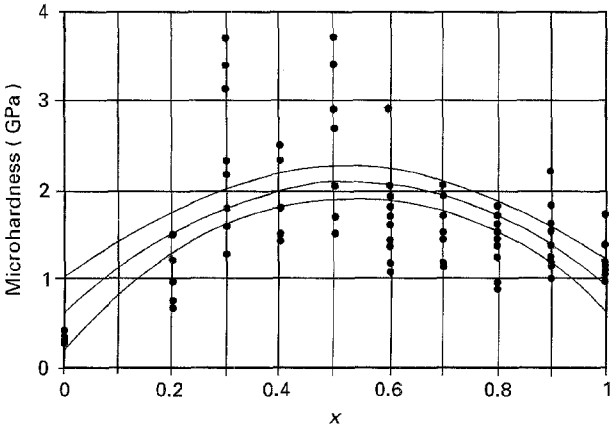

Figure 2 Microhardness, H, of the $Tl_xIn_{1-x}Se$ samples versus x. The best fit using Equation 1 is shown by the curve in the middle and the 95% confidence limits are shown as the upper and lower curves, respectively.

are "stopped" by the impurity atoms, due to the stronger bonds the latter are forming. We suppose that the formation of mixed crystals may be accompanied by such a decrease in dislocation density.

3. Analysis and discussion

One of the main reasons for the large statistical deviations in microhardness measurements on semiconductor compounds and their solid solutions is related to the lack of precise measuring methods due to their high brittleness in comparison with metals and alloys.

The study of a great number of solid solutions [6, 7] has shown that the microhardness dependence on composition in quasi-binary systems $A_xB_{1-x}C$ can be expressed by the following empirical equation, which holds also for many other physical quantities (like the bandgap, lattice parameter, etc.)

$$H(x) = H_A x + H_B(1 - x) + Kx(1 - x) \qquad (1)$$

where H_A and H_B are the values of the microhardness of the pure constituents of the solid solution, x, $1 - x$ are their corresponding concentrations in mole fractions and K a constant. To explain such variations of the properties of a mixed crystal, one has to recall the fact that the mole fraction, x, is a random variable bound to the limits $x = 0$ and $x = 1$ [10]. Composition fluctuations in a mixed crystal can be described by the deviation Δx of the fractional concentration of the A-type atoms which has an average value of x. If we choose a volume R^3 with linear size R, the average number of A-type atoms is $\bar{N}_A = N_A R^3$, and the total number of lattice sites is $\bar{N}N = NR^3$. The local deviation Δx in the concentration of the A-atoms (the fluctuation in composition) is given by

$$\Delta x = \Delta N_A / NR^3 = (xNR^3)^{1/2}/NR^3 \qquad (2)$$

The most simple assumption is that A- and B-type atoms in the solid solution are distributed in a completely random way. Then the random function $\Delta x(r) = [\bar{N}_A(r) - N_A]/\bar{N}$ which measures the local deviation in the concentration of A-type atoms in a small, but macroscopic, volume around point r will be a Gaussian random function of mean average equal to zero and with a pair correlation function

$$\langle \Delta x(r) \Delta x(r') \rangle = N^{-1} x(1 - x) \delta(r - r') \qquad (3)$$

where brackets denote averaging over the volume of the system, N is the concentration of all A- and B-type atoms and $\delta(r)$ is Dirac's delta function [10]. Now, for small fluctuations, one can expand the dependence

$$H[x(r)] = H(x) + [dH/dx]_x [x(r) - x] \qquad (4)$$

The second term has a Gaussian distribution with a mean average value equal to zero and a root–mean square fluctuation equal to

$$\sigma = |dH/dx| [x(1 - x)/\bar{N}]^{1/2} \qquad (5)$$

Already in this simple model one can describe semiempirically the bandgap bowing, proportional to $x(1 - x)$ (see, for example, [11]). Thus, we have tried to explain the variation of our experimental data as a function of x assuming that the microhardness and its standard deviation are given by Equations 1 and 5, respectively.

The fitting of our data by means of Equation 1 is shown in Fig. 2 (middle curve – the upper and lower curves being the 95% confidence limits). The maximum in the dependence is at $x = 0.53$, consistent with the assumed $x(1 - x)$ variation. The parameters of the curve $H(x) = a + bx + cx^2$ are listed in Table I, together with their standard error, t-value and 95% confidential limits, as well as other parameters evaluating statistical reliability of the model curve.

In contrast, the data on the standard deviation as a function of x shown in Fig. 3 cannot be explained assuming a dependence of the type of Equation 5. In fact, the experimental data show a maximum, whereas the prediction by means of Equation 5 has a minimum at compositions 0.4–0.5. We have found that using the log-normal distribution a much better fit can be obtained for both the microhardness and its standard deviation

$$f(x) = a + b \exp\{-0.5[\ln(x/c)/d]^2\} \qquad (6)$$

TABLE I Numeric summary for the best fit of $H(x)$ by means of a quadratic dependence (Equation 1) as shown in Figs 2 and 5

Rank 125 Eqn 1003 $y = a + bx + cx^2$

r^2 Coef det	DF adj r^2	Fit std err	F-value
0.3631692648	0.3406928859	0.6322438023	24.521866681

Parm	Value	Std error	t-value	95% confidence limits	
a	0.608008952	0.210676751	2.885980291	0.189216144	1.026801759
b	5.614307952	0.840007103	6.683643424	3.944503710	7.284112194
c	− 5.31725739	0.759529095	− 7.00072903	− 6.82708379	− 3.80743098

Area X_{min}–X_{max}	area precision		
1.6427437989	1.979984e-19		
Function min	X-value	Function max	X-value
0.6080089525	1.66924e-10	2.0899972912	0.5279326864
1st Deriv min	X-value	1st Deriv max	X-value
− 5.020206820	1.0000000000	5.6143079501	1.669243e-10
2nd Deriv min	X-value	2nd Deriv max	X-value
− 10.63451483	0.2619504842	− 10.63451464	0.5631963212

Soln vector	Covar matrix			
Direct	LUDecomp			
r^2 Coef det	DF adj r^2	Fit std err		
0.3631692648	0.3406928859	0.6322438023		
Source	Sum of squares	DF	Mean square	F
Regr	19.604361	2	9.8021803	24.5219
Error	34.376971	86	0.39973223	
Total	53.981332	88		

X variable: X

X_{min}:	0.0000000000	X_{max}:	1.0000000000	X_{range}:	1.0000000000
X_{mean}:	0.5820224719	X_{std}:	0.2933202554	X_{median}:	0.6000000000
$X@Y_{min}$:	0.0000000000	$X@Y_{max}$:	0.5000000000	$X@Y_{range}$:	0.5000000000

Y variable: microhardness (GPa)

Y_{min}:	0.2930000000	Y_{max}:	3.7200000000	Y_{range}:	3.4270000000
Y_{mean}:	1.6221011236	Y_{std}:	0.7832140373	Y_{median}:	1.5190000000
$Y@X_{min}$:	0.2930000000	$Y@X_{max}$:	1.3630000000	$Y@X_{range}$:	1.0700000000

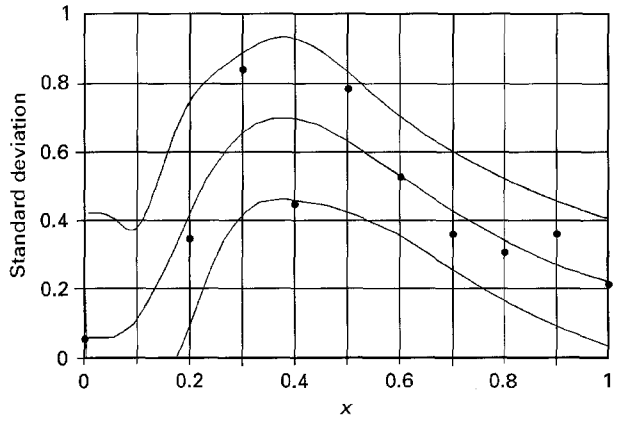

Figure 3 Experimental dependence of the standard deviation of H as a function of composition. The best fit is given by log-normal distribution (Equation 6) with 95% confidence limits shown by the upper and lower curves, respectively.

The corresponding parameters are given in Tables II and III, respectively, and the corresponding curves are shown in Fig. 3 for the standard deviation and in Fig. 4 for $H(x)$, together with their confidence limits. Finally, in Fig. 5 the predicted dependences according to Equations 1 and 6 for the microhardness are compared. The calculated values of four most frequently used statistical criteria obtained from the fit of microhardness data by means of Equations 1 and 6 are given in the first rows of Tables I and II respectively. The comparison shows that the log-normal distribution describes the experimental dependence $H(x)$ in a much better way according to all four criteria. In case of the standard deviation, the log-normal distribution is the best physically plausible fitting compared to a variety of about 320 different functional forms which have been tried.

One possible explanation of these results may be related to the fact that the monocrystalline materials of this family possess highly anisotropic mechanical and other properties in the direction of the c-axis and in a plane perpendicular to it. In fact, our specimens are polycrystalline with crystallites randomly oriented to the plane of the indentation. In addition, the environment where successive indentations have been produced is quite different due to different contents of impurities, defects, dislocations, etc. In our case, the random results of the experiment are expressed by means of the area of the indentation which is affected by many different and independent causes. If the effects of them were additive, the asymptotic distribution according to the Central Limit Theorem would be the Gaussian one and equations analogous to Equations 1 and 5 would be valid for the hardness and its standard deviation. However, the assumption that the interaction between different causes is expressed by simple addition is not always plausible. A much more natural assumption is that every cause produces some pulse, the result of which is proportional to the strength of the pulse itself. Let us suppose that we have n pulses, $R_1, R_2, \ldots, R_n$, which are independent

TABLE II Numeric summary for the best fit of the standard deviation of microhardness by means of log-normal distribution, as shown in Fig. 3

Rank 1 Eqn 8005 $y = a + b\exp\{-0.5[\ln(x/c)/d]^2\}$ (log-normal)

r^2 Coef det	DF adj r^2	Fit std err	F-value
0.7349451771	0.5229013188	0.1522455281	5.5456087842

Parm	Value	Std error	t-value	95% confidence limits	
a	0.055443217	0.148554950	0.373216892	−0.30957134	0.420457776
b	0.644373725	0.167704662	3.842312539	0.232306382	1.056441068
c	0.376769410	0.044404413	8.484954251	0.267663270	0.485875550
d	0.594999379	0.173369504	3.431972550	0.169012945	1.020985813

Area X_{min}–X_{max}	area precision
0.4237358415	4.258404e-10

Function min	X-value	Function max	X-value
0.0554432166	0.0010178024	0.6998169418	0.3767693954
1st Deriv min	X-value	1st Deriv max	X-value
−1.041522173	0.5872161156	3.4834031641	0.1696689692
2nd Deriv min	X-value	2nd Deriv max	X-value
−21.80618559	0.2644376475	41.737971396	0.0889373823

r^2 Coef det	DF adj r^2	Fit std err
0.7349451771	0.5229013188	0.1522455281

Source	Sum of squares	DF	Mean square	F
Regr	0.38562002	3	0.12854001	5.54561
Error	0.1390722	6	0.023178701	
Total	0.52469223	9		

X variable: X

X_{min}:	0.0000000000	X_{max}:	1.0000000000	X_{range}:	1.0000000000
X_{mean}:	0.5400000000	X_{std}:	0.3204163958	X_{median}:	0.5500000000
$X@Y_{min}$:	0.0000000000	$X@Y_{max}$:	0.3000000000	$X@Y_{range}$:	0.3000000000

Y variable: microhardness (GPa)

Y_{min}:	0.0528000000	Y_{max}:	0.8420600000	Y_{range}:	0.7892600000
Y_{mean}:	0.4262860000	Y_{std}:	0.2414521406	Y_{median}:	0.3643000000
$Y@X_{min}$:	0.0528000000	$Y@X_{max}$:	0.2162000000	$Y@X_{range}$:	0.1634000000

TABLE III Numeric summary for the best fit of $H(x)$ by means of log-normal distribution, as shown in Figs 4 and 5

Rank 9 Eqn 8005 $y = a + b\exp\{-0.5[\ln(x/c)/d]^2\}$ (log-normal)

r^2 Coef det	DF adj r^2	Fit std err	F-value
0.4924053889	0.4682342169	0.5677679028	27.485488840

Parm	Value	Std error	t-value	95% confidence limits	
a	0.388310213	0.211996011	1.831686412	−0.03317448	0.809794906
b	1.944326059	0.231663235	8.392898673	1.483739527	2.404912590
c	0.396279869	0.022906725	17.29971737	0.350737342	0.441822395
d	0.639357395	0.086340097	7.405103985	0.467698367	0.811016423

Area X_{min}–X_{max}	area precision
1.5859052865	1.601936e-09

Function min	X-value	Function max	X-value
0.3883102130	0.0006147410	2.3326362717	0.3962799668
1st Deriv min	X-value	1st Deriv max	X-value
−2.691100115	0.6320473221	9.8761445873	0.1650914073
2nd Deriv min	X-value	2nd Deriv max	X-value
−55.92070746	0.2633109703	118.85652470	0.0808750802

r^2 Coef det	DF adj r^2	Fit std err
0.4924053889	0.4682342169	0.5677679028

Source	Sum of squares	DF	Mean square	F
Regr	26.580699	3	8.8602329	27.4855
Error	27.400633	85	0.32236039	
Total	53.981332	88		

X variable: X

X_{min}:	0.0000000000	X_{max}:	1.0000000000	X_{range}:	1.0000000000
X_{mean}:	0.5820224719	X_{std}:	0.2933202554	X_{median}:	0.6000000000
$X@Y_{min}$:	0.0000000000	$X@Y_{max}$:	0.5000000000	$X@Y_{range}$:	0.5000000000

Y variable: microhardness (GPa)

Y_{min}:	0.2930000000	Y_{max}:	3.7200000000	Y_{range}:	3.4270000000
Y_{mean}:	1.6221011236	Y_{std}:	0.7832140373	Y_{median}:	1.5190000000
$Y@X_{min}$:	0.2930000000	$Y@X_{max}$:	1.3630000000	$Y@X_{range}$:	1.0700000000

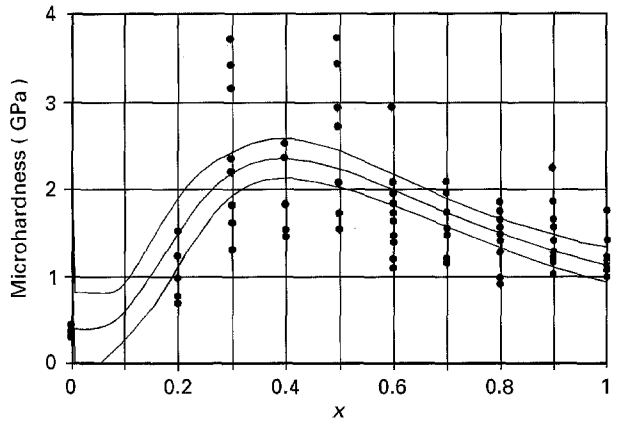

Figure 4 The data from Fig. 2 are fitted by means of log-normal distribution (Equation 6) with 95% confidence limits shown by the lower and upper curves, respectively.

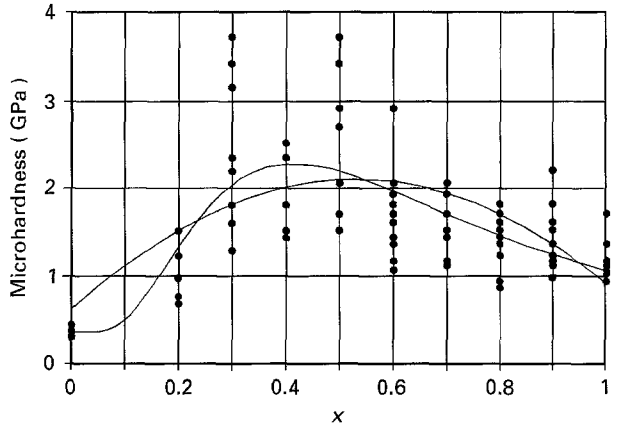

Figure 5 Comparison of the best fits from Figs 2 and 4 using curves of Equations 1 and 6.

random variables and let them affect the random variable X_0 (with an initial value X) so that after the action of $R_1 \ldots R_\nu$, it successively had the values $X_1 \ldots X_\nu$, respectively. Furthermore, suppose the increase in X due to the $(\nu + 1)$th pulse is proportional to $R_{\nu+1}$ and to some function $g(X_\nu)$ of the value of X after the νth pulse

$$X_{\nu+1} = X_\nu + R_{\nu+1} g(X_\nu) \quad (7)$$

If every pulse has changed the value of X only slightly, then approximately we would have

$$R_1 + R_2 + \cdots + R_n = \sum_0^{n-1} \frac{X_{\nu-1} - X_\nu}{g(X_\nu)} \approx \int_{x0}^{x} \frac{dt}{g(t)} \quad (8)$$

where $X = X_n$ is the final value of the variable. Since the R_js are independent, their sum is a Gaussian random variable. In the case $g(t) = t$ (the effect of each pulse is proportional to the value of X at moment t) one finds that $\log(X)$ is normally distributed, i.e. X obeys the log-normal distribution (Equation 6). Using the above mechanism, first proposed by the Dutch astronomer Kapteyn, Kolmogorov [12] has shown that the size of the crushed ores obeys a log-normal distribution.

4. Conclusions

In conclusion, it seems unlikely that, as a rule, the dependence of microhardness on composition obeys Equation 1, which is intuitively the most natural empirical law in solid solutions. We have found that in the system $Tl_xIn_{1-x}Se$, $H(x)$ is better described by the log-normal distribution, Equation 6, with a maximum at x ca. 0.5. Results obtained on similar systems, e.g. $(TlGaTe_2)_x$-$(TlGaS_2)_{1-x}$ and $(TlGaSe_2)_x$-$(TlInS_2)_{1-x}$, also show a pronounced maximum at x ca. 0.5 [13] in accordance with Kurnakov's rules. Concerning the member with $x = 0.5$, i.e. $TlInSe_2$, measurements of the Knoop hardness, H_K (reported in [14]), gave values for H_K in the range 0.7–0.74 GPa, not very different from those reported in the present work.

Acknowledgements

This work has been supported by the Scientific Research Foundation of St Kliment Ohridski University of Sofia, under Contracts 201/1993 and 165/1994, and by the Commission of the EC by contract CIPA CT-93/0255.

References

1. M. HANIAS, A.N.ANAGNOSTOPOULOS, K. KAMBAS and J. SPYRIDELIS, *Physica B* **160** (1989) 154.
2. *Idem. Phys. Rev. B* **43** (1991) 4135.
3. M. HANIAS and A. N. ANAGNOSTOPOULOS, *ibid.* **47** (1993) 4261.
4. M. P. HANIAS, J. A. KALOMOIROS, C. H. KARAKOTSOU, A. N. ANAGNOSTOPOULOS and J. SPYRIDELIS, *ibid.* **49** (1994) 16994.
5. CH. KARAKOTSOU and A. N. ANAGNOSTOPOULOS, *Mater. Res. Bull.* submitted.
6. N. A. GORYUNOVA, A. S. BORSHCHEVSKII and D. N. TRETIAKOV in "Semiconductors and semimetals: physics of III–V compounds", Vol. 4, edited by R. K. Willardson and A. C. Beer (Academic Press, New York, 1968) p. 3.
7. N. S. KURNAKOV, in "Selected works", Vol. 2 (in Russian) (Acad. Sci. USSR, Leningrad, 1965) p. 36.
8. Y. SEKI, J. MATSUI and H. WATANABE, *J. Appl. Phys.* **47** (1976) 3374.
9. Y. SEKI, H. WATANABE and J. MATSUI, *ibid.* **49** (1978) 822.
10. I. S. SHLIMAK, A. L. EFROS and I. Y. YANCHEV, *Sov. Phys. Semiconductors* **11** (1977) 149.
11. J. A. VAN VECHTEN and T. K. BERGSTRESSER, *Phys. Rev. B* **1** (1970) 3351.
12. A. N. KOLMOGOROV, *C.R. Acad. Sci. USSR*, **31** (1941) 99.
13. P. G. RUSTAMOV, S. G. ABDULLAEVA, O. M. ALIEV, M. M. GODZHAHEV, A. I. NADZHAFAROV and F. M. SEIDOV, *Izvest. Acad. Nauk SSSR-Neorg. Mater.* **19** (1983) 479.
14. T. J. ISAACS and R. P. HOPKINS, *J. Cryst. Growth* **29** (1975) 121.

Received 20 February
and accepted 24 May 1995